

## **Stimulated Radiation Interaction of a Single Electron Quantum Wavepacket**

Avraham Gover, Yiming Pan

*Department of Electrical Engineering Physical Electronics,*

*Tel Aviv University, Ramat Aviv 69978, ISRAEL*

### **Abstract**

We analyze the stimulated (emission/absorption) interaction of a single electron quantum wavepacket with coherent radiation, using perturbation theory and numerical solution of Schrodinger equation. The analysis applies to a wide class of free electron radiative interaction schemes, and is exemplified for Smith-Purcell radiation. Contrary to spontaneous emission, stimulated radiative interaction depends on the wavepacket characteristics in a certain range. When the electron drifts is beyond a critical length, dimension-dependent acceleration/deceleration of the wavepacket is fundamentally impossible because of the wavepacket spread. Below this range, such acceleration is possible, approaching the limit of classical “point particle” linear acceleration, when the wavepacket dimension is small relative to the radiation wavelength. Our analysis emulates the FEL gain in the limit of negligible recoil, and the quantum momentum recoil sidebands characteristics of PINEM - when recoil effect is significant. We use the platform for discussing the fundamental physics question of measurability of the quantum wavepacket size.

When interacting with a radiation wave under the influence of an external force, free electrons can emit radiation spontaneously, or be stimulated to emit/absorb radiation and get decelerated/accelerated. Such an interaction can also be facilitated without an external force when the electron passes through polarizable medium. Numerous spontaneous radiative emission schemes of both kinds are well known: Synchrotron radiation, Undulator radiation, Compton Scattering, Cerenkov radiation, Smith-Purcell radiation, transition radiation [1-6]. Some of these schemes were demonstrated to operate as coherent stimulated radiative emission sources, such as Free Electron Lasers (FEL) [7-9], as well as accelerating (stimulated absorption) devices, such as Dielectric Laser Accelerator (Inverse Smith-Purcell effect) [10]. In principle, all free electron spontaneous radiation emission schemes can be turned into stimulated emission devices, because of the fundamental Einstein relations between spontaneous emission and stimulated emission/absorption [11].

All of these spontaneous and stimulated radiation schemes have been analyzed in the classical limit - where they are modeled as point particles, and in the quantum limit - where they are normally modeled as plane waves [11-12]. Though some electron wavepacket features were considered in the context of infinite interaction length spontaneous Cerenkov radiation emission [13] there is no existing quantum wavepacket theory of stimulated radiative interaction that encompasses the quantum plane wave limit [14], the classical point particle limit and the intermediated finite wavepacket regime.

The interpretation and the essence of the electron quantum wavepacket and its electromagnetic interactions have been a subject of confusion and debate since the early conception of quantum mechanics. Modern QED theory and experiments indicate that spontaneous emission by a free electron is independent of its wavepacket dimensions [15-21]. However, in the present paper we focus on the stimulated emission process, and show that the wavepacket dimensions do affect the interaction in a certain range of operation.

The finite wavepacket, finite interaction length model presented here for free electron stimulated radiative interaction, leads to a distinction between two kinds of quantum effect conditions in single electron interaction: “the quantum recoil condition” and “the wavepacket significance condition”. The first condition relates to the significance of the electron quantum recoil relative to the momentum uncertainty in a finite interaction length. The second condition relates to whether the electrons interact with the radiation as a point particle with a determined phase or as an extended wave. This condition, contrary to common experience, assigns significance to the wavepacket size at the time of the radiative interaction and the history of its generation and transport to the interaction region.

## FIRST ORDER PERTURBATION ANALYSIS

Our one-dimensional interaction model is based on the first order perturbation solution of the relativistic “modified Schrödinger equation” [11]:

$$i\hbar \frac{\partial \psi(z, t)}{\partial t} = (H_0 + H_I(t))\psi(z, t), \quad (1)$$

where  $H_0 = \epsilon_0 + v_0(-i\hbar\nabla - p_0) + \frac{(-i\hbar\nabla - p_0)^2}{2m^*}$  is the free space Hamiltonian,  $m^* = \gamma_0^3 m$ , and the interaction part is:

$$H_I(t) = -\frac{e\hbar}{2\gamma_0 m \omega} \left\{ e^{-i(\omega t - \phi_0)} \tilde{E}(z) \cdot \nabla - e^{i(\omega t - \phi_0)} \tilde{E}^*(z) \cdot \nabla \right\}, \quad (2)$$

This model is fitting for discription of the variety of interaction schemes mentioned, where  $\tilde{E}(z) = E_0 e^{iq_z z} \hat{e}_z$  represents the dominant component of the radiation wave. We exemplify our modeling here for a case of Smith-Purcell radiation (see Figure 1), for which the radiation wave is a Floquent mode:  $\tilde{E}(z) = \sum_m \tilde{E}_m e^{iq_m z}$  with

$q_{zm} = q_{z0} + m2\pi/\lambda_G$ ,  $\lambda_G$  is the grating period,  $q_{z0} = q\cos\Theta$ ,  $q = \omega/c$  and  $\Theta$  is the incidence angle of the radiation wave relative to the axial interaction dimension. The radiation with  $q_z = q_{zm}$  represents one of the space harmonics  $m$  that satisfies synchronism condition with the electron [6]:  $v_0 \cong \omega/q_{zm}$ . We note that the analysis would be similar for the Cerenkov interaction scheme with  $q_z = n(\omega)\cos\Theta$  and  $n(\omega)$  the index of refraction of the medium. Furthermore, the analysis can be straightforwardly extended to the case of FEL and other interaction schemes [11].

The solution of Schrodinger equation to zero order (i.e. free space propagation) is well known. Assuming that the initial wavepacket, which is emitted at some point  $z = -L_D$  near the cathode face at time  $t = -t_D$ , is a gaussian at its waist, then:

$$\psi^{(0)}(z, t) = \left(2\pi\sigma_{p_0}^2\right)^{-\frac{1}{4}} \int \frac{dp}{\sqrt{2\pi\hbar}} \exp\left(-\frac{(p-p_0)^2}{4\sigma_{p_0}^2}\right) e^{ip(z+L_D)/\hbar} e^{-iE_p(t+t_D)/\hbar} = \int \frac{dp}{\sqrt{2\pi\hbar}} c_p^{(0)} e^{-iE_p t/\hbar} |p\rangle, \quad (3)$$

where  $|p\rangle = e^{ipz/\hbar}$ . Note that  $L_D, t_D = L_D/v_0$  are the “effective” drift length and drift time of the wavepacket center, that are somewhat different from the geometric distance and drift time from the cathode face. This is because of the initial section of electron acceleration from the cathode and because the wavepacket longitudinal waist may be somewhere within the cathode.

Expanding the energy dispersion relation to second order

$$E_p = c\sqrt{m^2c^2 + p^2} \approx E_0 + v_0(p - p_0) + \frac{(p - p_0)^2}{2m^*}, \quad (4)$$

The wavepacket development in momentum space is then given by

$$c_p^{(0)} = \left(2\pi\sigma_{p_0}^2\right)^{-\frac{1}{4}} \exp\left(-\frac{(p - p_0)^2}{4\tilde{\sigma}_p^2(t_D)}\right) e^{i(p_0 L_D - E_0 t_D)/\hbar}, \quad (5)$$

with

$$\begin{aligned}
\tilde{\sigma}_p^2(t_D) &= \sigma_{p_0}^2 \left(1 + i t_D / t_{R_{\parallel}}\right)^{-1}, \\
\sigma_{p_0} &= \hbar / 2 \sigma_{z_0}, \\
t_{R_{\parallel}} &= \frac{m^* \hbar}{2 \sigma_{p_0}^2} = 4 \pi \frac{\sigma_{z_0}^2}{\lambda_c^* c},
\end{aligned} \tag{6}$$

where we define

$$\lambda_c^* = \lambda_c / \gamma^3, \tag{7}$$

with  $\lambda_c = \hbar / mc$  – the Compton wavelength. The wavepacket development in space is calculated from Equation (3)

$$\psi^{(0)}(z, t) = \frac{\sqrt{\sigma_{z_0}}}{\left(2\pi\tilde{\sigma}_z^4(t+t_D)\right)^{1/4}} \exp\left(-\frac{(z-v_0 t)^2}{4\tilde{\sigma}_z^2(t+t_D)}\right) e^{i(p_0(z+L_D)-\varepsilon_0(t+t_D))/\hbar}, \tag{8}$$

Where  $t=0$  is the entrance time of the center of the wavepacket to the interaction region at  $z=0$  after a drift time  $t_D$ ,  $\tilde{\sigma}_z(t+t_D) = \sigma_{z_0} \sqrt{1 + i(t+t_D)/t_{R_{\parallel}}}$ . The wavepacket probability distribution

$$\left|\psi^{(0)}(z, t)\right|^2 = \frac{1}{\sqrt{2\pi\sigma_z^2(t+t_D)}} \exp\left(-\frac{(z-v_0 t)^2}{2\sigma_z^2(t+t_D)}\right), \tag{9}$$

displays particle propagation at velocity  $v_0 = \beta_0 c = p_0 / \gamma_0 m$  with wavepacket expansion:

$$\sigma_z(t) = |\tilde{\sigma}_z(t)| = \sigma_{z_0} \sqrt{1 + t^2/t_{R_{\parallel}}^2}. \tag{10}$$

The parameter  $t_{R_{\parallel}}$  is the evolution time from the waist for which  $\sigma_z(t_{R_{\parallel}}) = \sqrt{2}\sigma_{z_0}$ , in analogy to the Rayleigh length of wave diffraction. We now solve Equation (1) using the first order perturbation theory in momentum space

$$\psi(z, t) = \psi^{(0)}(z, t) + \psi^{(1)}(z, t) = \int \frac{dp}{\sqrt{2\pi\hbar}} \left( c_p^{(0)} + c_p^{(1)} \right) e^{-iE_p t/\hbar} |p\rangle. \quad (11)$$

Integration of Equation (1) in momentum space for  $c_p^{(1)}$  produces energy conserving terms of single photon emission/absorption corresponding to the two terms in the perturbation Hamiltonian:

$$c_{p'}^{(1)(e,a)} = \frac{\pi}{2i\hbar} \int dp \langle p' | H_I^{(e,a)} | p \rangle c_p^{(0)} \delta\left(\frac{E_p - E_{p'} \mp \hbar\omega}{2\hbar}\right), \quad (12)$$

Expanding again the energy dispersion relation (4) to second order, the delta function determines the quantum momentum recoil

$$p_{rec}^{(e,a)} = \left| p^{(e,a)} - p \right| = \frac{\hbar\omega}{v_0} (1 \pm \delta),$$

$$\delta = \frac{\hbar\omega}{2m^* v_0^2} \quad (13)$$

The first order perturbation momentum component is then

$$c_{p'}^{(1)(e,a)} = \frac{\pi}{iv_0} \langle p' | H_I^{(e,a)} | p \mp p_{rec}^{(e,a)} \rangle c^{(0)} \left( p \mp p_{rec}^{(e,a)} \right), \quad (14)$$

where the zero-order coefficient  $c_p^{(0)}$  is given in equation (5). The matrix element is straightforwardly calculated by

$$\begin{aligned} \langle p' | H_I^{(e,a)} | p \rangle &= \int \frac{dz}{2\pi\hbar} H_I^{(e,a)}(0) e^{i(p-p')z/\hbar} \\ &= \pm \frac{ieE_0 L_I p}{4\pi\gamma_0 m \hbar \omega} \text{sinc} \left( \frac{(p - p' \mp \hbar q_z) L_I}{2\hbar} \right) e^{i(p - p' \mp \hbar q_z) z / 2\hbar} e^{\pm i\phi_0}, \end{aligned} \quad (15)$$

and then simplified to

$$\langle p' | H_I^{(e,a)} | p \mp p_{rec}^{(e,a)} \rangle = \pm \left( \frac{iv_0}{\pi} \right) \Upsilon \left( \frac{p \mp p_{rec}^{(e,a)}}{p_0} \right) \text{sinc} \left( \frac{\bar{\theta}_{e,a}}{2} \right) e^{i \frac{\bar{\theta}_{e,a}}{2} \mp i\phi_0}, \quad (16)$$

with

$$\Upsilon = \frac{eE_0 L_I}{4\hbar\omega},$$

$$\bar{\theta}_{e,a} = \bar{\theta} \pm \frac{\varepsilon}{2},$$
(17)

where  $\bar{\theta} = \left( \frac{\omega}{\nu_0} - q_z \right) L_I$  is the classical “interaction detuning parameter”[9] and

$\varepsilon = \delta \left( \frac{\omega}{\nu_0} \right) L_I = 2\pi\delta L_I / \beta_0 \lambda$  is the interaction–length quantum recoil parameter[11].

We now can calculate the electron momentum density distribution after interaction:

$$\begin{aligned} \rho(p') &= \rho^{(0)}(p') + \rho^{(1)}(p') + \rho^{(2)}(p') \\ &= \frac{\left| c^{(0)}(p') \right|^2 + 2\text{Re}\left\{ c^{(1)*}(p') c^{(0)}(p') \right\} + \left| c^{(1)}(p') \right|^2}{\int dp' \left( \left| c^{(0)}(p') \right|^2 + \left| c^{(1)}(p') \right|^2 \right)}, \end{aligned}$$
(18)

where

$$\rho^{(0)}(p') = \left| c^{(0)}(p') \right|^2 = \left( 2\pi\sigma_{p_0}^2 \right)^{-\frac{1}{2}} \exp \left( -\frac{(p-p_0)^2}{2\sigma_{p_0}^2} \right),$$
(19)

is the initial Gaussian momentum density distribution. The second and third terms are given by

$$\begin{aligned} \rho^{(1)}(p') &= \frac{2\text{Re}\left\{ c_{p'}^{(1)(e)*} c_{p'}^{(0)} + c_{p'}^{(1)(a)*} c_{p'}^{(0)} \right\}}{\int dp' \left( \left| c^{(0)}(p') \right|^2 + \left| c^{(1)}(p') \right|^2 \right)} = \frac{2\Upsilon}{1 + \Upsilon^2 \left( \text{sinc}\left(\frac{\bar{\theta}_e}{2}\right) + \text{sinc}\left(\frac{\bar{\theta}_a}{2}\right) \right)} \times \\ &\quad \text{Re} \left\{ \left( \frac{p' - p_{rec}^e}{p_0} \right) \left( 2\pi\sigma_{p_0}^2 \right)^{-\frac{1}{2}} e^{-\frac{(p'-p_0)^2}{4\tilde{\sigma}_p^2(t_D)} - \frac{(p'-p_0-p_{rec}^e)^2}{4\tilde{\sigma}_p^2(t_D)}} \text{sinc}\left(\frac{\bar{\theta}_e}{2}\right) e^{i\left(\frac{\bar{\theta}_e}{2} - \phi_0\right)} \right. \\ &\quad \left. - \left( \frac{p' + p_{rec}^a}{p_0} \right) \left( 2\pi\sigma_{p_0}^2 \right)^{-\frac{1}{2}} e^{-\frac{(p'-p_0)^2}{4\tilde{\sigma}_p^2(t_D)} - \frac{(p'-p_0+p_{rec}^a)^2}{4\tilde{\sigma}_p^2(t_D)}} \text{sinc}\left(\frac{\bar{\theta}_a}{2}\right) e^{i\left(\frac{\bar{\theta}_a}{2} - \phi_0\right)} \right\}, \end{aligned}$$
(20)

and to second order in  $\Upsilon$  :

$$\begin{aligned} \rho^{(2)}(p') = & \Upsilon^2 \left[ \left( \frac{p' + p_{rec}^e}{p_0} \right)^2 \rho^{(0)}(p' + p_{rec}^e) - \rho^{(0)}(p') \right] \text{sinc}^2 \left( \frac{\bar{\theta}_e}{2} \right) \\ & + \Upsilon^2 \left[ \left( \frac{p' - p_{rec}^a}{p_0} \right)^2 \rho^{(0)}(p' - p_{rec}^a) - \rho^{(0)}(p') \right] \text{sinc}^2 \left( \frac{\bar{\theta}_a}{2} \right). \end{aligned} \quad (21)$$

### PHASE-INDEPENDENT MOMENTUM DISTRIBUTION

First we draw attention to the second order density distribution where the two terms in  $\rho^{(2)}$  display two side bands proportional to the initial density distribution  $\rho^{(0)}$  shifted centrally to  $p_0 \mp p_{rec}^{(e,a)}$  due to photon emission and absorption recoils (see Figure 2). Its first order moment results in the momentum acceleration/deceleration associated with stimulated radiative interaction:

$$\Delta p^{(2)} = \int \rho^{(2)}(p') p' dp' = \Upsilon^2 \left( \frac{\hbar \omega}{v_0} \right) \left[ \text{sinc}^2 \left( \frac{\bar{\theta}_e}{2} \right) - \text{sinc}^2 \left( \frac{\bar{\theta}_a}{2} \right) \right]. \quad (22)$$

Remarkably Equation (26) is independent of the wavepacket distribution  $\rho^{(0)}$ , and is satisfactorily consistent with the stimulated emission/absorption terms in the quantum-electrodynamic radiative emission expression for a single plane-wave electron wavefunction in the limit  $\rho^{(0)}(p') = \delta(p - p')$  that was derived in [11] for the photon emission rate:

$$\frac{dv_q}{dt} = \Gamma_{sp} \gamma_0 v_0 \left[ \left( v_q + 1 \right) \frac{1}{\gamma_e v_e} \text{sinc}^2 \left( \frac{\bar{\theta}_e}{2} \right) - v_q \frac{1}{\gamma_e v_e} \text{sinc}^2 \left( \frac{\bar{\theta}_a}{2} \right) \right]. \quad (23)$$

Using Equation (22-23) in the conservation of energy and momentum relation,

$$\Delta p^{(2)} = - \frac{L_I}{v_0} \left( \frac{\hbar \omega}{v_0} \right) \left( \frac{dv_q}{dt} \right)_{st}, \quad (24)$$



We can relate the interaction parameter  $\Upsilon$  (Equation (17)) to the spontaneous radiation emission coefficient  $\Gamma_{sp}$

$$\Upsilon^2 = \frac{L_I}{v_0} \Gamma_{sp} v_q, \quad (25)$$

and derive an explicit expression for the spontaneous emission rate per mode  $\Gamma_{sp}$  from the relation between  $v_q$  and  $|E_0|^2$ .

It is also interesting to point out that in the limit of negligible recoil relative to the finite-length homogeneous line broadening [11]:  $\varepsilon = \pi \frac{\hbar\omega}{m^* v_0^2} \frac{L_I}{\beta_0 \lambda} \ll 1$ ,

$$\Delta p^{(2)} = \frac{\hbar\omega}{v_0} \Upsilon^2 \varepsilon \frac{d}{d\bar{\theta}} \sin^2(\bar{\theta}/2), \quad (26)$$

consistently with the conventional classical gain expression of Smith-Purcell Cerenkov – FEL, as well as other FELs[9]. In particular it is instructive to note that the coefficient  $\Upsilon^2 \varepsilon$  scales like  $L^3$ . This is explained in FEL theory as a three stage gradual process of energy bunching of an ensemble of point particles, followed by density bunching and subsequent classical radiation emission. We have found that FEL interaction can take place even with a single electron, and it involves a process of bunching of the electron quantum wavepacket.

It should be noted that second order acceleration/deceleration (26) and FEL gain are only possible out of synchronism ( $\bar{\theta} \neq 0$ ) and are direct consequence of the nonlinearity of the electron energy dispersion relation. In practice the interaction recoil is negligible -  $\varepsilon \ll 0$ , and  $\bar{\theta}_e = \bar{\theta}_a = \bar{\theta}$ . Also the relative momentum recoil shift (13) is usually negligible -  $\delta = \hbar\omega/2m^* v_0^2 \ll 1$ , and therefore  $p_{rec}^{(e)} = p_{rec}^{(a)} = p_{rec}^{(0)}$ . Consequently the momentum distribution  $\rho^{(2)}$  (Eq. 21) is symmetric around  $p_0$ , and there is no net acceleration for  $\bar{\theta} = 0$ .

In Fig. 2 we show the momentum distribution after interaction (Eq. 21) for the case of when the quantum recoil momentum  $p_{\text{rec}}^{(0)}$  is significant relative to the wavepacket momentum spread

$$p_{\text{rec}}^{(0)} = \frac{\hbar\omega}{v_0} \gg \sigma_{p_0}, \quad (27)$$

The distribution shows distinct symmetric sideband spaced by  $p_{\text{rec}}^{(0)}$  on both sides of the center initial momentum  $p_0$ . Similar sideband development is shown in video1 based on numerical solution of Eq. 1 for weak interaction  $\Upsilon < 1$ . This result is similar to measured spectrum in PINEM experiments[22,23], where multiple sidebands were observed due to multiple photon emission, absorption. In our case of weak interaction only two emission/absorption sidebands are observed. Our Smith-Purcell first order perturbation analysis is directly applicable also to PINEM experiments with the substitution  $\bar{\theta} = 0$ . This is because in these experiments the near field interaction length is short relative to a wavelength, and therefore  $\bar{\theta} = \omega L_I / v_0 = 2\pi L_I / \beta_0 \lambda \ll 1$ .

In the classical limit of small recoil (opposite of (27)) the multiple photon emission/absorption sidebands degenerate into a symmetric continuous broadening of the momentum probability distribution, which is the reason why only energy spectral broadening and no net acceleration have been observed in DLA (stimulated Smith-Purcell) experiments[10].

It is necessary to realize that the conventional technology of electron energy spectroscopy necessitates averaged measurement of a multitude of electrons, in order to view the momentum distribution. If the electrons are emitted from a cathode unfiltered, then even if all emitted wavepacket are identical in their dimension, still the ensemble average involves convolution with the initial (thermal) momentum distribution of single electron emission

$$\rho_{en} = \int \rho^{(0)}(p', p_0) f\left(\frac{p_0 - p_{0,en}}{\sigma_{p,th}}\right) dp_0, \quad (28)$$

(see Figure 2). This, necessarily, results in widening of the measurable standard deviation of the Gaussian distribution of the ensemble to  $\sigma_{p,en}$  :

$$\sigma_{p,en}^2 = \sigma_{p,th}^2 + \sigma_{p_0}^2. \quad (29)$$

Since the measurable distribution satisfies  $\sigma_{p,en} > \sigma_p$ , the wavepacket broadening cannot be distinguished from the thermal distribution that determines the so called “Coherence time” of electron microscopes  $t_{coh} = \hbar / 2\sigma_{E,en}$  (typically  $\sigma_{E,en} < 0.7eV$ ). However, the quantum recoil effect on the momentum distribution of both emission and absorption (Equation (21)) is still observable if  $p_{rec}^{(0)} > \sigma_{p,en}$  as shown in Figure 2.

## PHASE-DEPENDENT MOMENTUM DISTRIBUTION

The second order perturbation term lost the dependence on the phase  $\phi_0$  of the wavepacket center relative to the laser field, and therefore does not reveal any specific features of the single electron wavepacket. We now draw attention to the first order density distribution (Equation (20)). This term has not been considered in previous analyses, but it is most interesting, because it retains the dependence on the phase  $\phi_0$ . In the limit of negligible recoil  $\varepsilon = 0$ , one obtains from first order expansion in terms of  $\delta$ :

$$\rho^{(1)}(p') = \frac{2\pi\Upsilon e^{-\Gamma^2/2} \text{sinc}\left(\frac{\bar{\theta}}{2}\right)}{1 + 2\Upsilon^2 \text{sinc}^2\left(\frac{\bar{\theta}}{2}\right)} \cos\left(\frac{\bar{\theta}}{2} - \phi_0 + \varphi\right) \left|C_{p'}^{(0)}\right|^2 \left( (p' - p_{rec}^e) e^{-\left(\frac{p' - p_0}{2\sigma_{p_0}^2}\right) p_{rec}^e + \delta \Gamma^2} - (p' + p_{rec}^a) e^{-\left(\frac{p' - p_0}{2\sigma_{p_0}^2}\right) p_{rec}^a - \delta \Gamma^2} \right), \quad (30)$$

where

$$\begin{aligned}\varphi &= \frac{2\omega t_D}{mv_0}(p' - p_0), \\ \Gamma &= \frac{\omega}{v_0} \sigma_z(t_D) = \frac{2\pi\sigma_z(t_D)}{\beta\lambda}.\end{aligned}\quad (31)$$

The decay coefficient  $e^{-\Gamma^2/2}$  assures that the first order term of the momentum distribution  $\rho^{(1)}$  is diminished when  $\Gamma \gg 1$ , namely when the wavepacket expands on its way from the source beyond the size of the interaction wavelength.

To first order in  $p_{\text{rec}}^{(0)}$ , we get

$$\rho^{(1)}(p') = \frac{4\left(\frac{\hbar\omega/v_0}{p_0}\right) \Upsilon \rho^{(0)}(p') \text{sinc}\left(\frac{\bar{\theta}}{2}\right) e^{-\Gamma^2/2}}{1 + 2\Upsilon^2 \text{sinc}^2\left(\frac{\bar{\theta}}{2}\right)} \cos\left(\frac{\bar{\theta}}{2} + \phi_0 + \varphi\right) \left[1 + \frac{\Gamma^2 p'}{2m^* v_0} - \frac{(p' - p_0)p'}{2\sigma_{p_0}^2}\right]. \quad (32)$$

Neglecting  $\varphi$ , the momentum transfer is:

$$\begin{aligned}\Delta p^{(1)} &= \int \rho^{(1)}(p') p' dp' = \frac{\frac{2}{\gamma_0^2} \frac{\hbar\omega}{v_0} \Upsilon \text{sinc}\left(\frac{\bar{\theta}}{2}\right) \Gamma^2 e^{-\Gamma^2/2}}{\left(1 + 2\Upsilon^2 \text{sinc}^2\left(\frac{\bar{\theta}}{2}\right)\right)} \cos\left(\phi_0 + \frac{\bar{\theta}}{2}\right) \\ &\simeq \frac{\Gamma^2 e^{-\Gamma^2/2}}{2\gamma_0^2} \frac{eE_0 L_I}{v_0} \text{sinc}\left(\frac{\bar{\theta}}{2}\right) \cos\left(\phi_0 + \frac{\bar{\theta}}{2}\right),\end{aligned}\quad (33)$$

for  $\Upsilon \ll 1$ . This expression can be contrasted with the classical “point particle” momentum transfer equation

$$\Delta p_{\text{point}} = \frac{eE_0 L_I}{v_0} \text{sinc}\left(\frac{\bar{\theta}}{2}\right) \cos\left(\phi_0 + \frac{\bar{\theta}}{2}\right).$$

and the corresponding expression for stimulated-superradiant emission energy  $W_q = \nu_0 \Delta p_{point}$  [24]. Except for the decay factor the acceleration/deceleration of the quantum wavepacket scales with  $\bar{\theta}$  and  $\phi_0$  similarly to the case of a point particle.

$$\Delta p^{(1)} / \Delta p_{point} = \Gamma^2 e^{-\Gamma^2/2} / 2\gamma_0 \quad (34)$$

Figures 3 and 4 display the momentum density distribution  $\rho^{(0)} + \rho^{(1)}$  for the case  $\bar{\theta} = 0$  and acceleration phase:  $\phi_0 = 0$ . The resultant post-interaction distribution gets lopsided towards positive momentum. The peak distribution is shifted about  $\Delta p^{(1)} = \frac{2}{\gamma_0^2} \frac{\hbar\omega}{\nu_0} \Upsilon$  for  $\Gamma = \sqrt{2}$ . A left shifted momentum distribution would appear in the case of deceleration for phase  $\phi_0 = \pi$ . Larger shift is not to be expected in our first order perturbation theory (classical acceleration/deceleration involves multiphoton exchange and requires complete high order perturbation analysis of Equation (1) or numerical computation [25]). Video 2 displays significant nearly “point-particle-like” classical acceleration, based on numerical computation solution of Eq. 1.

## WAVEPACKET DEPENDENT STIMULATED INTERACTION

Of great curiosity is the effect of the wavepacket expansion factor  $\Gamma$  in Equation (32-33). Evidently the “point particle” limit (34) does not evolve from Equation (33) in the limit  $\Gamma \ll 1$  ( $\sigma_z(t_D) \ll \lambda\beta_0$ ) as might be expected. Figure 5 shows that the decay factor  $\Gamma^2 e^{-\Gamma^2/2}$  diminishes in the limits  $\Gamma \rightarrow 0$ ,  $\Gamma \rightarrow \infty$ , it reaches a maximum value  $2/e$  when  $\Gamma = \sqrt{2}$ . Substitution of Equation (6) in Equation (10) results in the relation

$$\sigma_z(t_D) = \sqrt{\sigma_{z0}^2 + \left( \frac{\lambda_c^*}{4\pi} \frac{ct_D}{\sigma_{z0}} \right)^2}, \quad (35)$$

It is obvious that  $\sigma_{z_0} \rightarrow 0$  is not the point particle limit, since then the wavepacket size explodes. Moreover,  $\sigma_z(t_D)$  cannot be arbitrarily small, it has an absolute minimum for any given  $t_D$ , independently of  $\sigma_{z_0}$

$$\sigma_z(t_D)|_{\min} = \sqrt{\frac{\lambda_c^*}{2\pi} ct_D}, \quad (36)$$

This corresponds to a minimum value of  $\Gamma$  for fixed frequency  $\omega$

$$\Gamma_{\min} = \frac{\omega}{v_0} \sqrt{\frac{\lambda_c^*}{2\pi} ct_D}, \quad (37)$$

We define a critical drift length  $z_G = v_0 t_{DG}$  as the distance for which  $\Gamma_{\min} = \sqrt{2}$

$$z_G = \frac{\beta_0^3 \gamma_0^3}{\pi} \frac{\lambda^2}{\lambda_c}, \quad (38)$$

We come to the significant observation that for drift distances away from the source  $L_D \gg z_G$ , wavepacket-dependent linear (in the field) acceleration/deceleration of a single electron is diminished, because the wavepacket inevitably spreads wider than the interacting wavelength, and the wavepacket center phase is undefined, even if one can determine accurately the wavepacket emission time relative to the wave phase  $\phi_0$  at the interaction region. This observation is also consistent with an earlier suggestion that the quantum wavepacket spread poses a fundamental physical high frequency limit or short wavelength limit  $\lambda_{\text{cutoff}} = (\pi \lambda_c / \beta^3 \gamma^3)^{1/2}$  on measurement of particle beam shot-noise, challenging the conventional mathematical “point-particle” model presentation of shot-noise as an unbound “white noise” [26].

The diminishing of the linear field acceleration due to the  $\Gamma^2 e^{-\Gamma^2/2}$  factor is quite understandable in the limit  $\Gamma \gg \sqrt{2}$  that corresponds to wavepacket spread beyond the accelerating field wavelength  $\sigma_z(t_D) \gg \beta_0 \lambda$ , On the other hand, the diminishing

acceleration effect in the limit  $\Gamma(t_D) \ll 1$  due to the factor  $\Gamma^2 e^{-\Gamma^2/2}$  (that is not forbidden in the range  $L_D < z_G$ ) is in contradiction to the intuitive expectation that in this limit,  $\sigma_z(t_D) \ll \beta_0 \lambda$ , the wavepacket would accelerate as a point particle. However we must point out that this result was derived within the framework of first order perturbation theory, where only single photon recoil is involved in the radiative interaction.

The phase-dependent linear field acceleration regime  $\Delta p^{(1)}$  is of fundamental interest, because contrary to the second order acceleration  $(p^{(2)}, \Delta p^{(2)})$ , its characteristics depend on the wavepacket dimensions. So far, previous laser acceleration experiments of single electrons [10,22] were carried out only in the second order acceleration regime, where only broadening of the momentum spectrum is possible without net acceleration.

Inspection of Equation (33) indicates that maximum acceleration (or deceleration) would take place for  $\bar{\theta} = 0, \phi_0 = 0(\text{or } \pi), \Gamma(t_D) = \sqrt{2}$  :

$$\Delta p_{\max}^{(1)} = \frac{4}{e\gamma_0^2} \Upsilon p_{\text{rec}}^{(0)}, \quad (39)$$

where  $\Upsilon$  - the number of exchanged photons (Equation (17)) must satisfy  $\Upsilon < 1$  in the first order approximation, and  $p_{\text{rec}}^{(0)} = \hbar\omega/v_0$ . Therefore, net acceleration is achievable, but because

$$\Gamma(t_D) > \Gamma(t_D = 0) = \Gamma_0 = \frac{\omega}{v_0} \sigma_{z_0} = \frac{p_{\text{rec}}^{(0)}}{\sigma_{p_0}}, \quad (40)$$

therefore the acceleration  $\Delta p_{\max}^{(1)}$  is smaller than the wavepacket momentum spread  $\sigma_{p_0}$  and the relative shift of the momentum distribution is marginally observable (as displayed in Figure 3). The relative shift may however be larger than 1 in the multiphoton exchange regime where  $\Upsilon \gg 1$ .

The effect of the wavepacket size on the acceleration of a single electron wavepacket in the weak interaction limit can be identified if one varies the parameter  $\Gamma = 2\pi\sigma_z(t_D)/\beta_0\lambda$  over a range near  $\Gamma \leq \sqrt{2}$ , and measure a dependence of the wavepacket acceleration (34) as in Fig. 5 and dependence on the laser phase  $\phi_0$  as in (33). Experimentally one can scan over  $\Gamma(t_D), \sigma_z(t_D)$  (Eq. (35)) by performing the radiative interaction at different drift distances  $L_D = v_0 t_D$ , as long as one keeps  $L_D < z_G(\lambda, \beta_0)$ . Also it is possible to vary  $\lambda, \beta_0$  and interact repeatedly with the same electron.

A measurement of acceleration at different distances and wavelengths is analogous to measurement of the transverse diffraction characteristics of a laser beam of wavelength  $\lambda$  by measuring its transmission through apertures of radius  $R$  at different distances  $L$  from the beam waist. Such measurements reveal information about the beam, if made at distances shorter than the aperture Rayleigh length  $z_R = \pi R^2 / 2\lambda$ . In the stimulated emission experiments the interaction wavelength  $\beta_0\lambda$  acts as a moving longitudinal aperture (analogous to the diffraction aperture  $R$ ) with  $\lambda^* / \beta$  playing the same role as the optical wavelength  $\lambda$  in the diffraction experiment.

Controlled sub-femtosecond single electron photo emission and phase synchronized interaction with radiation field are possible at infrared up to THz beam wavelengths [27-30]. Taking for example typical electron microscope energy of 120keV and energy spread  $\sigma_E = 0.7eV$ , the ensemble coherence length is 0.07 $\mu m$ . With energy filtering [31] down to  $\sigma_E = 0.02eV$  a coherence length as long as 2.5 $\mu m$  is expected. The electron wavepackets, that are longer from the coherence length at birth, expand further significantly after drift from the cathode, primarily in the low energy acceleration section of the gun. Yet, with wavelengths in the IR to THz regime one may expect possible experimental conditions for stimulated radiative interaction in the wavepacket-dependent acceleration regime discussed here.



Measurement of the electron momentum distribution requires accumulation of data from an ensemble of particles emitted from the electron source. Measurements of the wavepacket characteristics of electrons photo-emitted from single-electron emission sources like a tip [32] or an ion cold-trap [33] would be usually masked by random (thermal) spread of the particles in the ensemble. Because of the ensemble random (thermal) momentum spread, after a short drift length, the statistical spatial spread of the ensemble exceeds the size of the individual wavepackets [34]. This limits the practical range within which the stimulated interaction experiment can be carried out, unless the electron beam source is very cold and a protected weak measurements of Aharonov-Vaidman's kind [35] could be employed.

In conclusion, the semiclassical first order perturbation analysis presented here shows that stimulated interaction of a single electron wavepacket with radiation (contrary to spontaneous emission) can be dependent on the features of the wavepacket and its spatial position relative to the phase of the accelerating wave. This can only happen in a certain range, close enough to the electron emission source. Previous experiments, both PINEM experiments, in the quantum-recoil-dominated regime, and DLA experiments, in the classical negligible-quantum-recoil regime, operated out of the range where wavepacket dependent acceleration could be significant, and therefore they all displayed only symmetric momentum broadening of the interacting electrons without net acceleration. We showed, however, that due to the nonlinearity of the electron energy dispersion relation, net second order (in the field) acceleration is still possible at any drift length, when the symmetry of emission/absorption is broken in an extended interaction length. In this case, the stimulated radiative interaction of a single electron is the same as in a multi-particle classical FEL, and is entirely independent of the wavepacket entrance position relative to the radiation phase.

**Acknowledgements** We acknowledge Yakir Aharonov, A. Friedman, S. Rushin and Amnon Yariv for useful discussions and comments. The work was supported in parts by DIP (German-Israeli Project Cooperation) and US-Israel Binational Science Foundation, and by the PBC program of the Israel council of higher education.

**Author Contributions** A.G. conceived and supervised the project. Y.P. performed modeling and numerical calculation of the electron wavepacket with the near-field interaction. A.G. and Y.P. co-wrote the paper with all authors contributing to discussion and preparation of the manuscript. Correspondance and requests for materials should be addressed to A. G. ([gover@eng.tau.ac.il](mailto:gover@eng.tau.ac.il)) or Y.P. ([yimingpan@mail.tau.ac.il](mailto:yimingpan@mail.tau.ac.il)).

**Competing interests statement** The authors declare no competing financial interest.

## References

1. Brau, Charles A. Modern Problems in Classical Electrodynamics. *Oxford University Press*, ISBN 0-19-514665-4 (2004).
2. H. Motz, "Applications of the radiation from fast electron beams", *J. Appl. Phys.* **22**, 527-535 (1951).
3. V. P. Sukhattmee, P. W. Wolff, "Stimulated Compton scattering as a radiation source-Theoretical limitations", *J. Appl. Phys.* **44**, 2331-2334 (1973).
4. Cherenkov, P. A., "Visible emission of clean liquids by action of  $\gamma$  radiation". *Doklady Akademii Nauk SSSR*. **2**, 451(1934).
5. V. L. Ginzburg and I. M. Frank, "Transition radiation," *Zh. Eksp. Teor. Fiz.* **16**, 15–22 (1946).
6. S. J. Smith and E. M. Purcell, "Visible light from localized surface charges moving across a grating," *Phys. Rev.* **92**, 1069 (1953).
7. J. M. Madey, "Stimulated emission of bremsstrahlung in a periodic magnetic field," *Appl. Phys.* **42**, 1906-1913 (1971).
8. Pellegrini, C., A. Marinelli, and S. Reiche. "The physics of x-ray free-electron lasers." *Reviews of Modern Physics* **88(1)**, 015006 (2016).
9. Gover, A., and P. Sprangle. "A unified theory of magnetic bremsstrahlung, electrostatic bremsstrahlung, Compton-Raman scattering, and Cerenkov-Smith-Purcell free-electron lasers." *IEEE Journal of Quantum Electronics* **17(7)**, 1196-1215 (1981).
10. Peralta, et al., Demonstration of electron acceleration in a laser-driven dielectric microstructure. *Nature* **503(7474)**, 91-94 (2013).
11. Friedman, A., Gover, A., Kurizki, G., Ruschin, S., & Yariv, A., Spontaneous and stimulated emission from quasifree electrons. *Reviews of Modern Physics* **60(2)**, 471 (1988).
12. Peter Kling et al., "What defines the quantum regime of the free-electron laser?" *New J. Phys.* **17**, 123019 (2015).

13. I. Kaminer, *et al.*, "Quantum Čerenkov radiation: spectral cutoffs and the role of spin and orbital angular momentum." *Phys. Rev. X* **6**, 011006 (2016).
14. I. P. Ivanov, "Quantum calculation of the Vavilov-Cherenkov radiation by twisted electrons" *Phys. Rev. A* **93**, 053825 (2016).
15. P. Krekora, R. E. Wagner, Q. Su, and R. Grobe, *Laser Phys.* **12**, 455 (2002).
16. E. A. Chowdhury, I. Ghebregziabihier, and B. C. Walker, *J. Phys. B* **38**, 517 (2005).
17. J. Peatross, J. P. Corson, and G. Tarbox, *Am. J. Phys.* **81**, 351 (2013).
18. A. Barut, *Found. Phys. Lett.* **1**, 47 (1988).
19. Ware, Michael, et al. "Measured photoemission from electron wave packets in a strong laser field." *Optics letters* **41(4)**, 689-692 (2016).
20. Peatross, Justin, et al. "Photoemission of a single-electron wave packet in a strong laser field." *Phys. Rev. Lett.* **100(15)**, 153601 (2008).
21. Corson, J.P., Peatross, J., Müller, C. and Hatsagortsyan, K.Z., 2011. Scattering of intense laser radiation by a single-electron wave packet. *Physical Review A*, 84(5), p.053831.
22. Feist, A. et al. Quantum coherent optical phase modulation in an ultrafast transmission electron microscope. *Nature* **521**, 200-203 (2015).
23. Herink, G., Solli, D. R., Gulde, M., & Ropers, C. "Field-driven photoemission from nanostructures quenches the quiver motion." *Nature*, **483(7388)**, 190-193 (2012).
24. Gover, A., Superradiant and stimulated-superradiant emission in prebunched electron-beam radiators. I. Formulation. *Physical Review Special Topics-Accelerators and Beams*, **8(3)**, 030701(2005).
25. Talebi, Nahid. "Schrödinger electrons interacting with optical gratings: quantum mechanical study of the inverse Smith–Purcell effect." *New Journal of Physics* **18(12)**, 123006 (2016).
26. R. Iancu, A. Gover, A. Nause, "spectral limits and frequency sum-rule of current and radiation noise measurement" *TUP007 Proceedings of FEL*, Basel, Switzerland (2014).

27. E. Curry, S. Fabbri, P. Musumeci and A. Gover, "THz-driven zero-slippage IFEL scheme for phase space manipulation" *New J. Phys.* **18**, 113045 (2016).
28. Herink, G., Wimmer, L., & Ropers, C. "Field emission at terahertz frequencies: AC-tunneling and ultrafast carrier dynamics." *New Journal of Physics*, **16(12)**, 123005(2014).
29. Ossiander, M., et al. "Attosecond correlation dynamics." *Nature Physics* **13**, 280-285(2017).
30. Kealhofer, C., Schneider, W., Ehberger, D., Ryabov, A., Krausz, F., & Baum, P. "All-optical control and metrology of electron pulses." *Science*, **352(6284)**, 429-433 (2016).
31. Krivanek, Ondrej L., Tracy C. Lovejoy, Niklas Dellby, and R. W. Carpenter. "Monochromated STEM with a 30 meV-wide, atom-sized electron probe." *Microscopy* **2013**, 089 (2013).
32. Michael Kruger, Markus Schenk, Peter Hommelhoff, "Attosecond control of electrons emitted from a nanoscale metal tip", *Nature* **475**: 78 -81 (2011).
33. W.J. Engelen, E.J.D. Vredenburg, O.J. Luiten, "Analytical model of an isolated single-atom electron source" *Ultramicroscopy* **147**, 61–69 (2014).
34. Ford, G. W., and R. F. O'Connell. "Wave packet spreading: Temperature and squeezing effects with applications to quantum measurement and decoherence." *American Journal of Physics* **70.3**: 319-324(2002).
35. Aharonov, Yakir, and Lev Vaidman. "The two-state vector formalism: an updated review." In *Time in quantum mechanics*, 399-447. Springer Berlin Heidelberg (2008).

## Figures

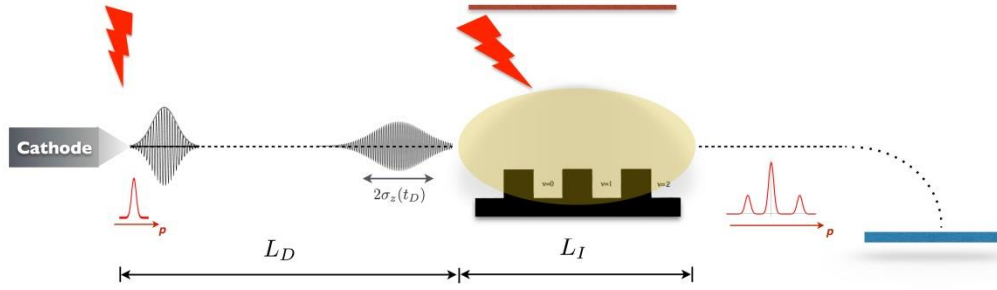


**Figure 1| The experiment setup.** Single electron wavepackets are photo-emitted from a cathode driven by an ultra-short pulse fs laser. After a free propagation length  $L_D$ , the expanded wavepacket passes next to the surface of a grating of length  $L_I$ , and interacts with the near-field radiation, that is excited by an IR wavelength laser, phase locked to the photo-emitting laser. The accelerated/decelerated momentum distribution of the modulated wavepacket is measured with an electron energy spectrometer.

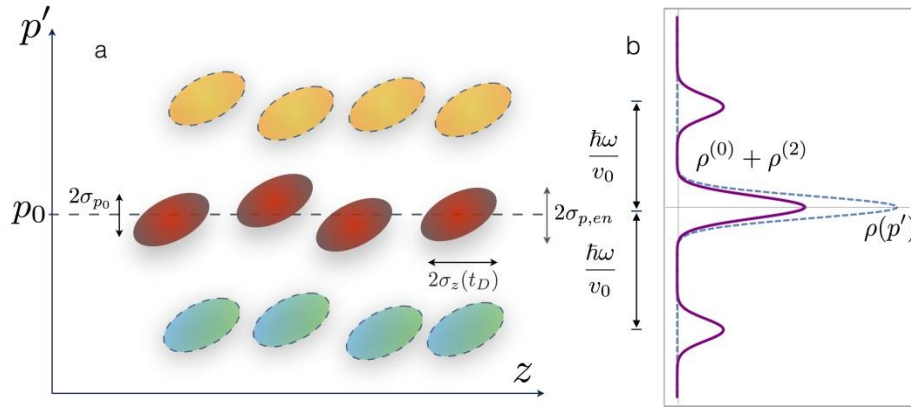


**Figure 2| The quantum recoil limit of electron-laser interaction.** The phase-space distribution of an ensemble of quantum wavepackets after interaction with the near-field is shown in (a), and its final momentum distribution is shown in (b). In this limit the

condition  $p_{rec} = \frac{\hbar\omega}{v_0} \gg \sigma_{en} > \sigma_{p0}$  is satisfied, where  $\sigma_{en}$  is the ensemble momentum spread.

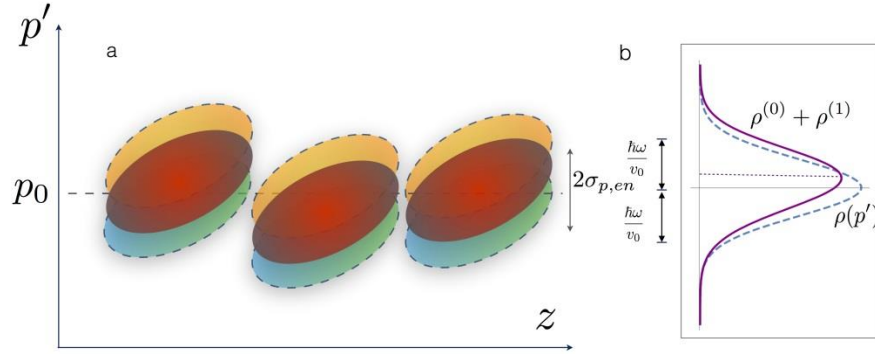


**Figure 3| Linear field acceleration of a phase-defined wavepacket.** The phase space distribution of electron quantum wavepackets interacting weakly with the near-field wave is shown in (a), and its final momentum distribution in (b). In this limit

$$\Gamma = \frac{2\pi\sigma_z(t_D)}{\beta\lambda} \simeq 1 \text{ and } p_{rec} = \frac{\hbar\omega}{v_0} \ll \sigma_{p0}.$$

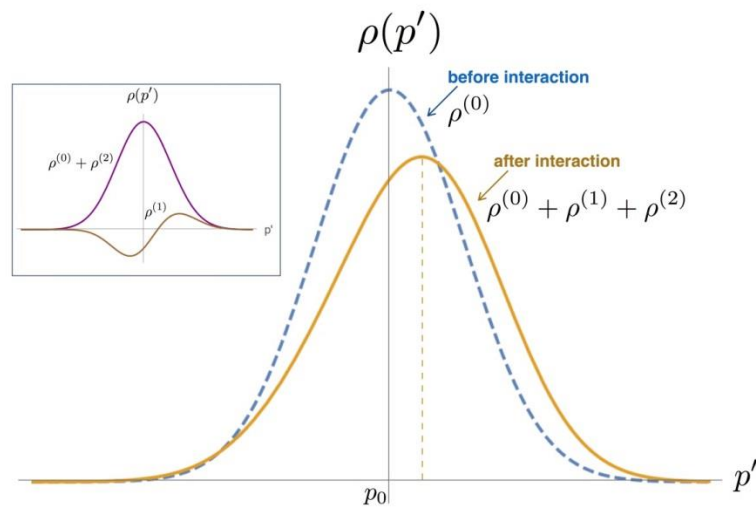


**Figure 4| Total final momentum distribution of a Linear field accelerated phase-defined wavepacket.** The parameters are for maximal momentum gain:  $\bar{\theta} = 0$  (velocity synchronizm),  $\phi_0 = 0$  (accelerating phase),  $\Gamma = \sqrt{2}$ . The inset shows the incremental distributions  $\rho^{(1)}$  and  $\rho^{(2)}$  seperately.

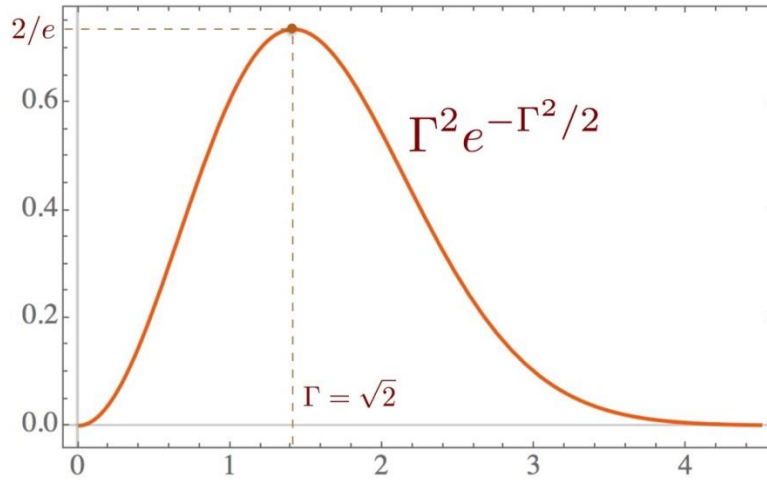


**Figure 5| The decay factor of wavepacket acceleration/deceleration relative to the “point-particle” classical case.** In both limits of short wavepacket ( $\Gamma \rightarrow 0$ ) and long wavepacket ( $\Gamma \rightarrow \infty$ ), the decay factor diminishes the acceleration/deceleration.



**Video-1:** Wavepacket evolution for the case  $\bar{\theta}=0$  weak field  $\Upsilon \ll 1, \sigma_{p0} < \hbar\omega/v_0, \sigma_z(t_D) > \lambda\beta_0$  with sidebands formation and no net acceleration:

a) Evolution in space - z (pink -  $\text{Im } \Psi(z)$  , blue-  $\text{Re } \Psi(z)$  , purple -  $|\Psi(z)|$  ).

b) Evolution in momentum  $\rho(p) = |c(p)|^2$  .

**Video-2:** Wavepacket evolution for the case  $\bar{\theta}=0, \phi_0=0(\pi)$  , and strong field  $\Upsilon \gg 1, \sigma_z(t_D) < \lambda\beta_0$  with net acceleration/deceleration:

a) Evolution in space- z.

b) Evolution in momentum  $\rho(p) = |c(p)|^2$  .